Journal of Mechanical Research and Application (JMRA), Vol. 15 No.3, 1404 (2025),70-84

JMRA
Journal of Mechanical Research and Application
ISSN: 2251-7383, eISSN: 2251-7391

An innovative retrofitting strategy incorporating phase change materials (PCMs) into air conditioning systems to enhance energy efficiency and reduce the overall energy demand of buildings.

AmirAli Mokhtari

Head of Mechanical equipment, EXEGER COMPANY

Abstract

Introducing fresh air into HVAC systems enhances indoor air quality but often increases energy consumption. This study presents a retrofitted HVAC configuration integrating a phase change material (PCM)-based heat exchanger to improve energy efficiency. Calcium chloride hexahydrate ($CaCl_2 \cdot 6H_2O$), selected via the TOPSIS method with entropy weighting, was used to pre-cool incoming air. The influence of PCM thickness (20–100 mm) and longitudinal fins (5 mm × 50 mm) on energy performance was analyzed under summer conditions in a composite climate using R134a. Results showed that 100 mm PCM with 48 fins achieved maximum peak and average energy savings of 12% and 9%, respectively. Thinner PC Ms with fewer fins yielded proportionally lower savings. The proposed approach demonstrates the potential of PCM-based retrofits for enhancing HVAC sustainability and reducing cooling energy demand in buildings.

Keywords:

HVAC, Energy Savings, TOPSIS, Air-phase change material heat exchanger, Retrofitting techniques

1. Introduction

Cooling is vital for economic growth, health, and productivity in hot climates, yet increased urban heat island effects raise energy demand—accounting for nearly 60% of total energy consumption in

buildings. The IEA predicts a 47 Mtoe rise in cooling demand by 2040 due to urban expansion and increased household AC penetration (from 0.6 to 1.6 units per household). Conventional HVAC systems improve air quality by mixing fresh and recirculated air, but the COVID-19 pandemic has driven authorities (e.g., ASHRAE, ISHRAE) to recommend higher fresh air intake—often at ambient temperatures up to 48 °C—further increasing energy use.

Phase Change Materials (PCMs) offer a promising solution by storing and releasing latent heat near their transition temperatures, enhancing building thermal regulation. While PCM integration into walls and heat exchangers has achieved load reductions up to 12%, conventional material selection often focuses narrowly on melting point and latent heat. This study instead applies the TOPSIS method to select an optimized PCM–air heat exchanger for fresh air pre-cooling, examining the effects of PCM thickness and fin configuration on HVAC energy efficiency.

2. Methodology

"This section outlines the methodologies applied to address the research statements, following the sequence presented in Figure 1."

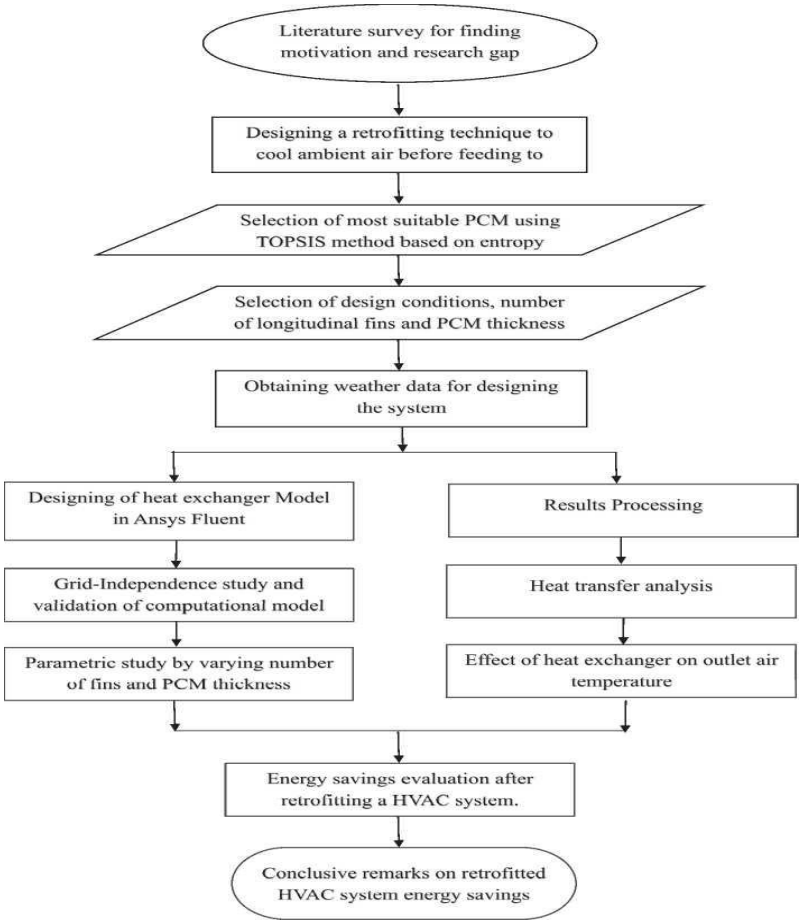

Figure 1. Flow Chart for the study

2.1. Material Selection

The selection of suitable commercial PCMs is often constrained by limited experimental data and expert judgment, which may result in suboptimal choices affecting system performance [36]. To overcome this, multi-attribute decision-making (MADM) methods—particularly TOPSIS—are employed to evaluate alternatives based on key thermophysical properties [37,38]. By incorporating entropy-based weighting, which objectively reflects data variability without human bias, the method enhances decision reliability [39]. This study applies entropy-weighted TOPSIS to select the most appropriate PCM with phase change temperatures between 27 °C and 32 °C, ensuring thermal comfort. Additional properties considered include latent heat, specific heat, thermal conductivity, and density in both solid and liquid states. Table 1 summarizes selected PCMs within the target temperature range.

Table 1. Selected PCMs with thermal properties [39,40].

S. No.	Material	Melting Temperature (°C)	Latent Heat (kJ kg^{i1})	Density (kg m^{i3})		Thermal Conductivity (W m^{i1} K^{i1})		Specific Heat (kJ $kg^{-1}K^{i1}$)	
				Solid	Liquid	Solid	Liquid	Solid	Liquid
1	Bio-PCMQ27	27	251.30	235.00	225.00	0.21	0.19	1.77	0.99
2	RT28HC	28	250.00	880.00	770.00	0.20	0.20	2.00	2.00
3	CaCl2·.6H2O	30	187.00	1710.00	1530.00	1.09	0.54	2.20	1.40
4	OM29	29	229.00	868.00	770.00	0.29	0.17	4.80	3.90
5	Bio-PCMQ29	29	260.70	235.00	225.00	0.21	0.19	2.22	0.27
6	Paraffin wax	32	251.00	830.00	830.00	0.51	0.22	1.92	3.26
7	Capric acid	32	152.70	878.00	878.00	0.37	0.14	0.47	0.47
8	RT31	31	165.00	880.00	760.00	0.20	0.20	2.00	2.00
9	n-Octadecane	27	243.50	865.00	860.00	0.19	0.15	2.14	2.66

The methodology uses m evaluation criteria (D_1 to D_m) and n performance indicators (X_1 to X_n), with the complete procedure detailed in Annexure I. Entropy-based TOPSIS was employed to calculate attribute weights (Figure. 2), revealing that thermophysical properties—beyond just melting temperature and latent heat—significantly influence PCM selection. Latent heat had the highest weight (0.37), followed by density in solid and liquid states (0.16), while phase change temperature received

the lowest weight due to its narrow range (27–32 °C). Thermal conductivity and specific heat were also included for their role in heat transfer.

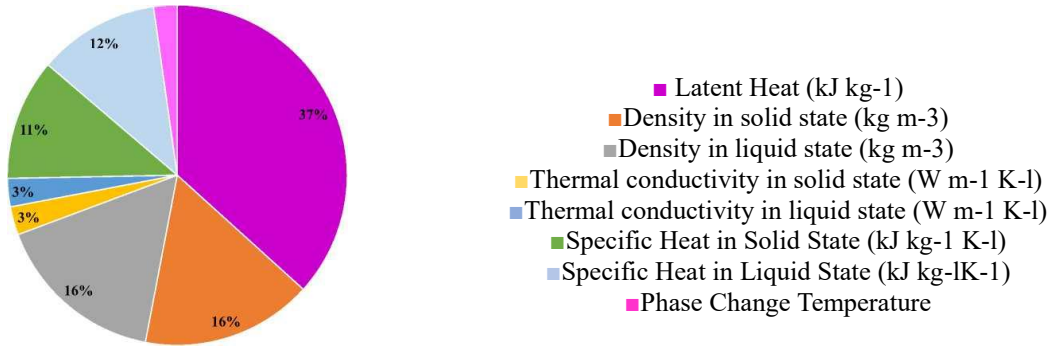

Figure۷ . Weight of attributes obtained by using TOPSIS entropy-based methodology.

A weight-normalized decision matrix (Table 2) was created to rank PCMs based on closeness to ideal and anti-ideal solutions. Calcium chloride hexahydrate emerged as the optimal PCM and is henceforth referred to simply as 'PCM'.

Table 2. Weight standardized decision matrix and ranking of PCM using TOPSIS.

S. No.	Material	Melting temperature	Latent Heat	Density Solid	Liquid	Thermal conductivity Solid	Thermal conductivity Liquid	Specific Heat Solid	Specific Heat Liquid	Si+	Si-	N^+	Rank
1	Bio-PCMQ27	0.0006	0.0067	0.0121	0.0119	0.0367	0.0284	0.0304	0.0340	0.0067	0.0121	0.644	8
2	RT28HC	0.0006	0.0067	0.0454	0.0408	0.0350	0.0299	0.0343	0.0687	0.0067	0.0454	0.871	6
3	CaCl2·.6H2O	0.0006	0.0050	0.0882	0.0810	0.1905	0.0806	0.0377	0.0481	0.0050	0.0882	0.946	1
4	OM29	0.0006	0.0061	0.0448	0.0408	0.0512	0.0257	0.0823	0.1340	0.0061	0.0448	0.88	4
5	Bio-PCMQ29	0.0006	0.0070	0.0121	0.0119	0.0367	0.0284	0.0381	0.0093	0.0070	0.0121	0.634	9
6	paraffin wax	0.0007	0.0067	0.0428	0.0440	0.0898	0.0334	0.0329	0.1120	0.0067	0.0428	0.865	7
7	Capric acid	0.0007	0.0041	0.0453	0.0465	0.0650	0.0210	0.0082	0.0163	0.0041	0.0453	0.917	2
8	RT31	0.0007	0.0044	0.0454	0.0402	0.0350	0.0299	0.0343	0.0687	0.0044	0.0454	0.912	3
9	n-Octadecane	0.0006	0.0065	0.0446	0.0455	0.0332	0.0221	0.0367	0.0914	0.0065	0.0446	0.873	5
	V+	0.0007	0.0070	0.0882	0.0810	0.1905	0.0806	0.0823	0.1340				
	V-	0.0006	0.0041	0.0121	0.0119	0.0332	0.0210	0.0082	0.0093				

Due to inconsistencies in literature, the selected PCM's melting temperature and latent heat were verified using a DSC-Q2000 (TA, USA), with ±0.01 °C accuracy. A GR-202 microbalance (A&D, Japan) was used to weigh samples. Tests were performed under nitrogen flow with a temperature range

of –10 °C to 60 °C at 1 °C/min. The PCM fully melted at 30.02 °C with a latent heat of 171.06 J/g. Characterization was repeated thrice for uncertainty analysis, yielding ±1.1% error in enthalpy and ±0.16 °C in phase change temperature. For simulation, 30 °C and 171 kJ/kg were used.

2.2. Physical Domain

The latent heat energy storage system (LHESS) is modeled as a vertical shell-and-tube exchanger (Figure 3) with a 1500 mm length. Air, serving as the heat transfer fluid, flows along gravity through an inner aluminum tube (200 mm diameter, 5 mm thickness), while the annular space contains $CaCl_2 \cdot 6H_2O$ PCM. To study the effect of PCM thickness on heat exchanger performance, it is varied as 20, 50, 75, and 100 mm, increasing the outer diameter up to 410 mm.

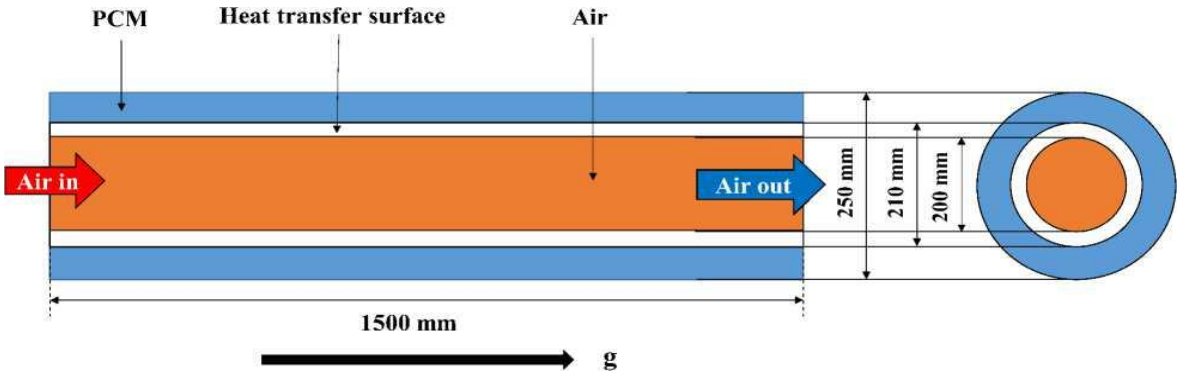

Figure3. Schematic layout of the physical domain of the designed LHESS.

Table 3 Thermophysical properties of CaCl2·6H2O and air [39,41].

Property	CaCl2·6H2O	Air
ρ(kg/m^3)	1538	1.225
k(W/m K)	0.546	0.0242
c_p (J/kg K)	2230	1006.43
μ(Pa.s)	0.01	1.789 x 10^{-5}
$T_{solidus}$ (°C)	30	–
$T_{solidus}$ (°C)	30	–
LI_{atent}(kJ/kg)	171	–

air's low thermal conductivity (Table 3), longitudinal fins are used to enhance heat transfer. Four configurations (6, 12, 24, and 48 fins) are tested; more than 48 causes fin overlap and flow

disruption. Fins are 5 mm wide and 50 mm high.

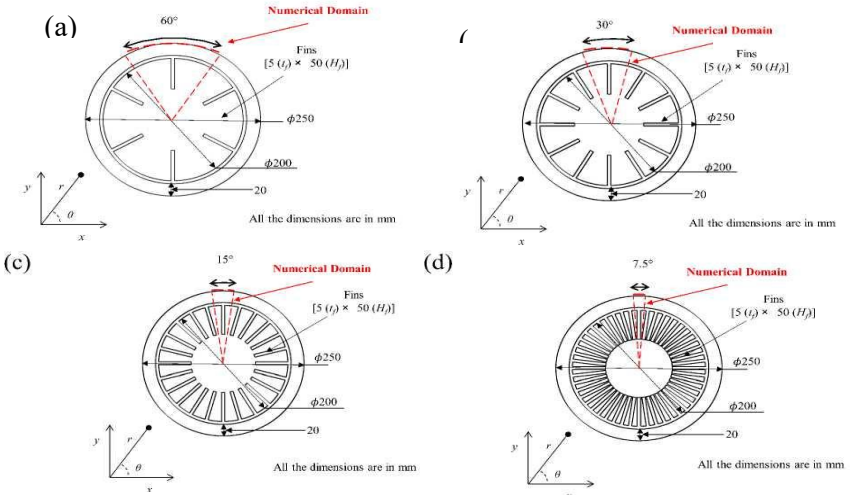

Figure 4. The physical and numerical domains of the heat exchanger with extended surfaces (fins) (a) 6 fins, (b) 12 fins, (c) 24 fins, and (d) 48 fins.

Due to the computational cost of full 3D modeling, symmetry-based domain simplification is adopted (Figure 4). For each fin configuration, the model is reduced to a fraction of the geometry: one-sixth for 6 fins, one-twelfth for 12, and so on. Symmetry and uniform radial heat transfer are assumed.

2.3. Numerical Modelling

2.3.1. Heat Exchanger

The transient, axisymmetric 3D model simulates LHESS behavior for different fin numbers. The melted PCM is treated as an incompressible, laminar, Newtonian fluid. Radiation, volume changes during phase transition, and viscous dissipation are neglected for simplification.

The thermophysical properties of air, tube material and PCM are assumed to be constant, except for the density of PCM, which is approximated using the Boussinesq approximation, which considers the buoyancy forces (F_B).

$$F_B = -\rho\beta\,(T_p - T_m) \quad (1)$$

Where ρ and Tm represent the density of the fluid PCM and phase change temperature, respectively, and β represents the coefficient of thermal expansion.

On incorporating the assumptions to the governing equations of continuity, momentum, and energy for modelling the transient heat transfer and laminar fluid flow of PCM are written as [41],

Continuity equation: $$\frac{\partial(\rho)}{\partial t} + \nabla.(\rho V) = 0 \quad (2)$$

Momentum equation: $$\frac{\partial(\rho V)}{\partial t} + V\nabla.(\rho V)$$

$$= -\nabla P + \nabla^2[\mu V] + S_z + \frac{(1-\lambda)^2}{\lambda^3+c} VA_{mush} \quad (3)$$

Energy equation: $\frac{\partial(\rho H)}{\partial t} + V\nabla.(\rho HV) = \nabla^2 [kT] + S_{tp}$ (4)

Where V represents the bulk velocity, Amush is the mushy zone and is influenced by the morphology of the porous medium, and c is a small number to prevent the term from achieving an indeterminant form. The source term expression in the momentum conservation equation for PCM indicates the implementation of the Boussinesq approximation along the z-axis. This approximation implies that all thermophysical properties, with the exception of fluid density, remain unaltered. The source term, therefore, can be represented as follows:

$S_z = \rho g\beta (T_p - T_m)$ (5)

To investigate the phase change behaviour of PCM in a heat exchanger, the enthalpy porosity technique with a fixed grid approach is used. According to it, the porous zone denotes the fraction of PCM that has changed its phase to liquid and is represented by a melt fraction(λ) [41] denoting that the value of λ for a melting process varies from a value of zero to one, where zero signifies the material is in the solid phase, while one indicates the complete melting of PCM and change of phase to liquid.

$$\lambda = \begin{cases} 0, T \leq T_s \\ \frac{T-T_s}{T_L-T_s}, T_s < T < T_L \\ 1, T \geq T_L \end{cases} \quad (6)$$

H represents the net thermal energy of PCM, represented by equation (7), while ΔH is for latent and sensible heat of the PCM and represented by equation (8), which are stated as,

$H = h + AH = h + \lambda\, h_{LH}$ (7)

$H = h_o + \int_{T_o}^{T} C_P AT$ (8)

2.3.2. Method of Solution

Numerical simulations were carried out in ANSYS FLUENT 2021 using the finite volume method. The SIMPLE algorithm handled velocity–pressure coupling, while the PRESTO scheme discretized pressure. Relaxation factors were set at 0.3 (pressure), 0.7 (momentum), and 0.7 (melt fraction). Convergence criteria were 10^{-3} for continuity and momentum, and 10^{-6} for energy.

2.3.3. Boundary and Initial Conditions

Ambient air temperature data were obtained from a weather station at IIT Delhi (accuracy ±0.2 °C) and defined as a time-dependent function replicating conditions on June 9, 2022. The inlet air flows through the heat exchanger, transferring heat to the PCM before entering the HVAC system, which regulates indoor air at 27 °C dry bulb temperature.

The mass of air required for cooling is estimated from the sensible load and enthalpy difference,

assuming 50% fresh air. Adiabatic mixing of recirculated and fresh air determines the mixed air enthalpy. Energy absorbed by the refrigerant is computed based on this enthalpy and supply conditions. Refrigerant mass flow and compressor work are calculated using energy balance and enthalpy differences across the evaporator. The compressor's efficiency is based on the pressure ratio, and total HVAC work is used to estimate energy savings after system retrofitting.

3. Grid Independence and Model Validation

Three grid sizes (354,806; 685,350; 1,211,560 cells) were tested with a 0.1 s time step. Results showed less than 1.2% variation in outlet air temperature between coarse and fine grids, and less than 0.6% between fine and finer grids.

The model was validated using results from Gau and Viskanta's [41] experiment and Brent et al.'s [41] simulation of gallium melting. Using similar boundary conditions and geometry, the present model showed good agreement in melt front progression, confirming its accuracy for PCM phase change modeling.

4. Results and Discussion

4.1. Air Outlet Temperature

Air outlet temperature was analyzed for different fin configurations (0–48 fins) and PCM thicknesses (20–100 mm). At 20 mm thickness, fins reduced the rate of temperature rise during PCM melting, but after 6 h, outlet temperatures converged (~42.3 °C) across all configurations. The 48-fin case achieved the highest average ΔT (2.29 °C), with only short-term benefits due to low PCM volume.

At 50 mm thickness, improved latent heat capacity led to reduced outlet temperatures, with 48 fins showing the largest drop (ΔT = 0.51 °C). As PCM thickness increased to 75 mm, thermal regulation improved further; 48 fins reduced the outlet temperature to 36.01 °C after 6 h. At 100 mm, temperature differences were 0.9 °C (no fins) to 4.6 °C (48 fins).

Thus, outlet air temperature can be reduced by increasing either the PCM thickness (latent heat capacity) or the number of longitudinal internal fins (heat transfer enhancement).

4.2. Melt Fraction

Figure 5 illustrates the temporal evolution of the PCM melt fraction for varying fin numbers and PCM thicknesses. The inlet air conditions correspond to Delhi's composite climate in June 2022. In Fig. 5(a), for 20 mm PCM thickness and upright orientation (gravity aligned with the tube axis), PCM melting begins at 450 s (no fin), 280 s (6 fins), 190 s (12 fins), 160 s (24 fins), and 100 s (48 fins). Increased fin count reduces melting time due to enhanced heat transfer area, with total melting

achieved in 3 h (no fins), 2.72 h (6), 2.5 h (12), 1.5 h (24), and 1 h (48 fins). The most notable performance gain occurs between 24 and 48 fins, although geometric constraints limit further fin addition.

At 50 mm PCM thickness [Fig. 5(b)], melting time increases due to the larger PCM volume. Full melting occurs at 5.25 h (no fins), 4.65 h (6), 4.42 h (12), 4.18 h (24), and 2.82 h (48 fins), demonstrating greater energy storage and prolonged cooling potential.

Given the HVAC operation period of 6 h, attention shifts to delayed PCM melting to sustain lower air outlet temperatures. For 75 mm thickness [Fig. 5(c)], after 6 h, melt fractions are 72.5% (no fins) and 87.15% (6 fins), with melting time reductions of 12.85%, 15.5%, and 36.95% for 12, 24, and 48 fins compared to the 50 mm case. This prolongs latent heat absorption and supports better thermal performance.

At 100 mm thickness [Fig. 5(d)], melt fractions after 6 h are 70.08% (6 fins), 77.55% (12), 85.56% (24), and 92.45% (48 fins). Full melting is not achieved, yet the 48-fin configuration improves melt fraction by 37.95% over the no-fin case. This suggests that complete melting is not essential for effective air temperature stabilization; instead, gradual melting offers superior thermal buffering over extended periods. Figure 6 presents the spatial extent of PCM melting (middle plane) for the 48-fin, 100 mm configuration at 1, 3, and 6 h. Ambient air enters at z=1500z = 1500z=1500 mm. After 1 h, 18% of PCM is melted; by 6 h, 92.45% is molten, with solid PCM mainly at the bottom corner. The melting front rises over time (to 1125 mm at 3 h), forming a trapezoidal pattern due to stratified heat transfer and natural convection. These findings affirm that adjusting PCM thickness and fin count can effectively modulate melting behavior and heat exchanger performance.

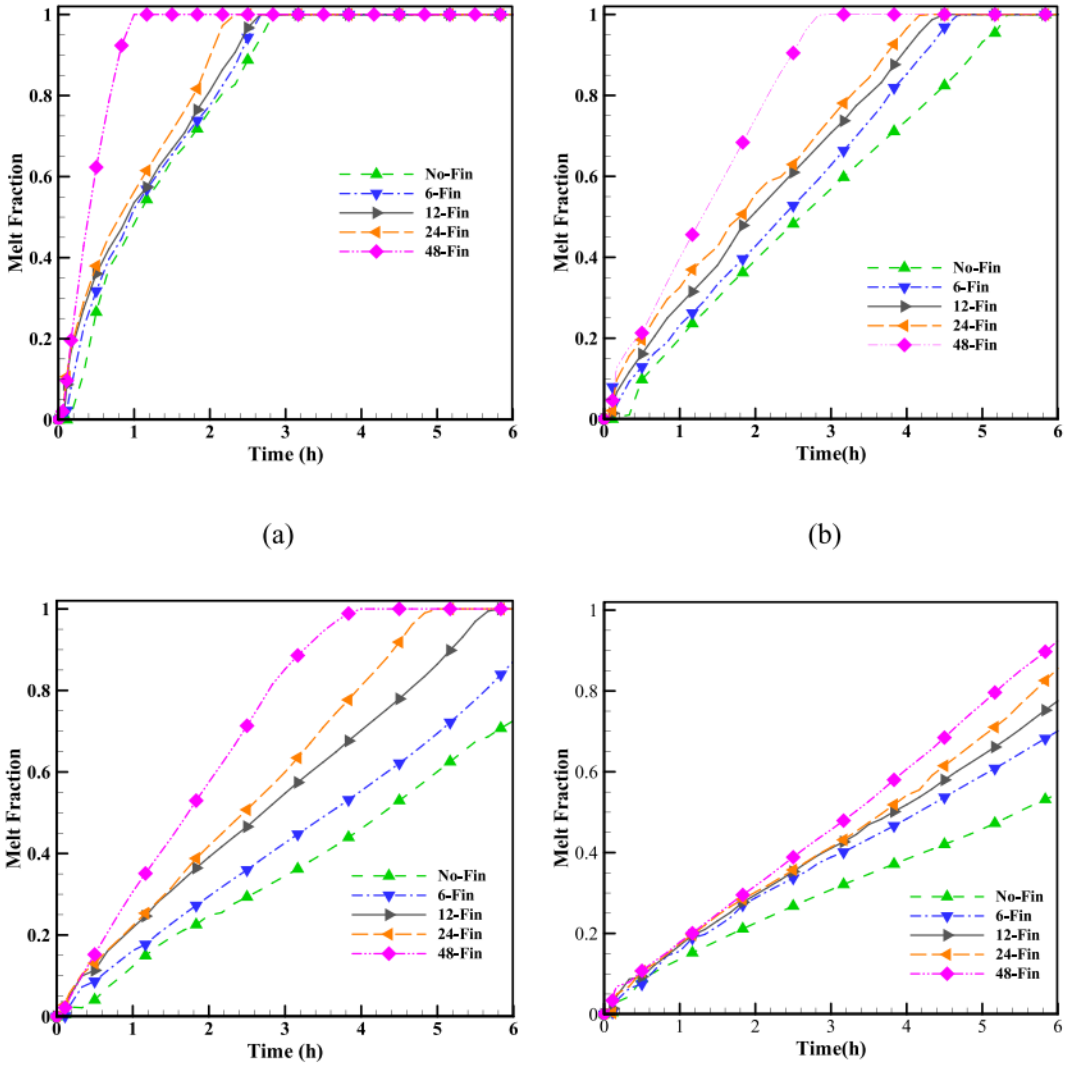

Figure 5. Temporal variation of melting fraction with varying number of fins for PCM thickness of (a) 20 mm, (b) 50 mm, (c) 75 mm and (d) 100 mm.

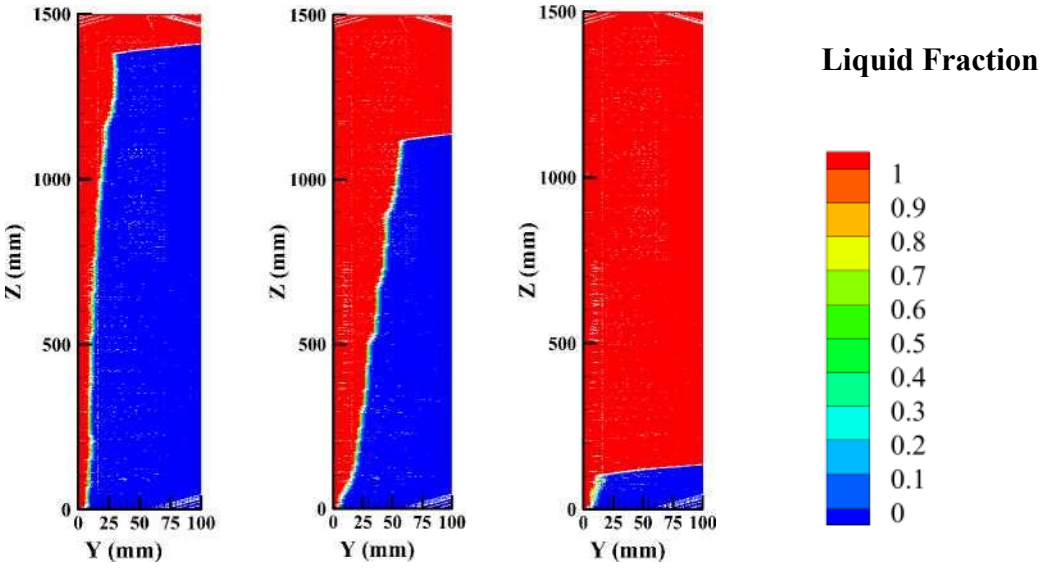

Fig. 6. Melt fraction of 48 finned heat exchanger with PCM thickness of 100 mm at (a) 1 h, (b) 3 h, (c) 6 h

4.3. Energy Savings (Condensed & Paraphrased)

Energy savings from retrofitting HVAC systems with a PCM-based heat exchanger were evaluated against a conventional setup. Figure 7and Table 4 show energy savings over 6 hours of operation with varying fin counts and PCM thicknesses.

At 20 mm PCM thickness, the 12-fin configuration achieved the highest average energy savings (3.22%), while the no-fin setup achieved the least (1.75%). Increasing the fin count beyond 12 led to diminishing returns due to faster PCM melting.

Table 4 Energy savings in percentage achieved by retrofitted HVAC system

Thickness	No fin	6 fins	12 fins	24 fins	48 fins
20 mm	1.75	2.10	**3.22**	2.63	2.24
50 mm	2.15	3.18	4.88	**5.22**	4.92
75 mm	2.79	4.22	5.64	5.57	**6.64**
100 mm	2.88	4.45	6.15	6.76	**9.06**

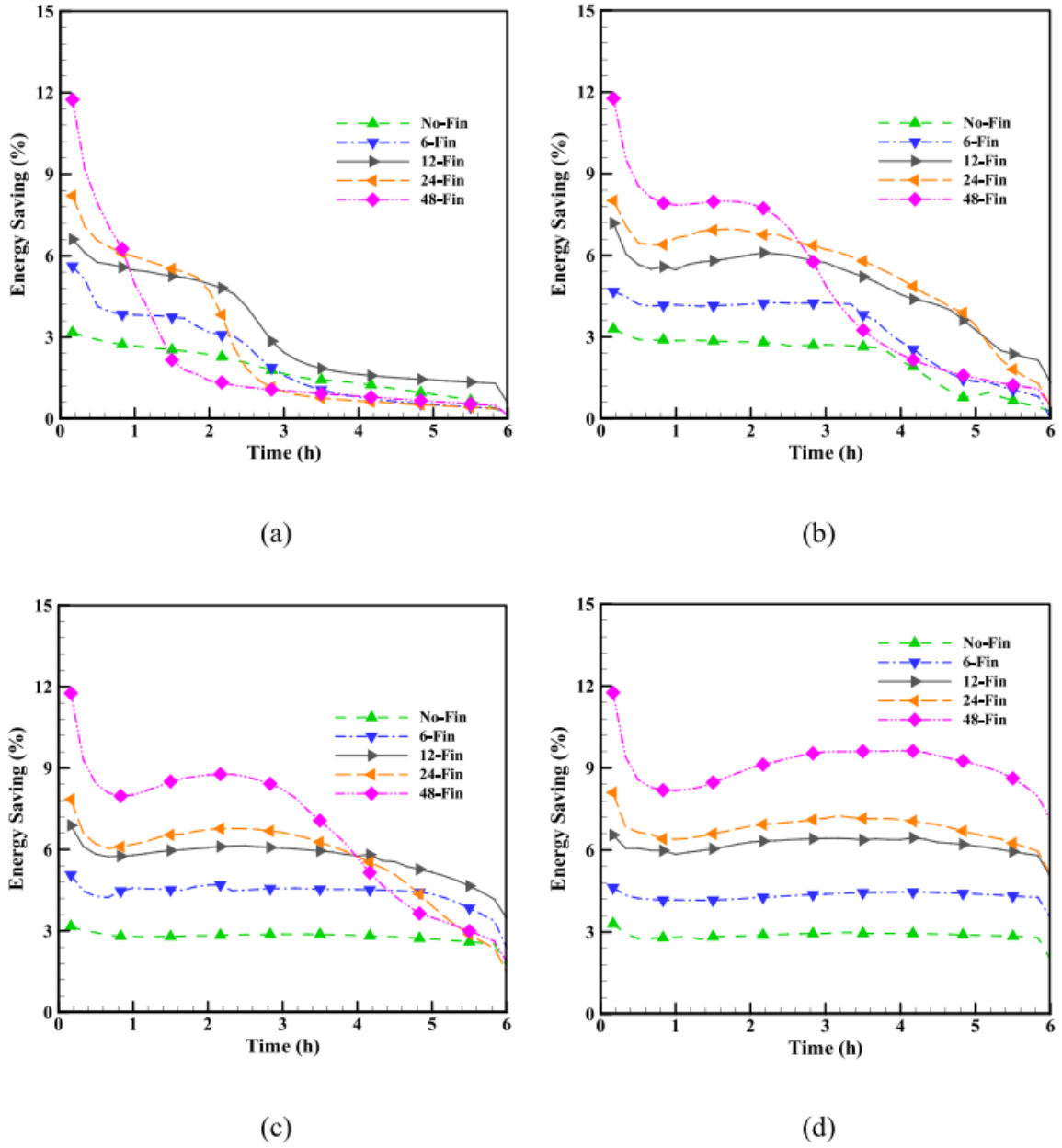

Figure 7. Temporal variation of Energy saving by varying number of fins for PCM thickness of (a) 20 mm, (b) 50 mm, (c) 75 mm and (d) 100 mm.

With 50 mm PCM, the 24-fin configuration yielded the highest savings (5.22%). Thicker PCM delayed complete melting, allowing prolonged latent heat storage and better performance. At 75 mm, the best results (6.64%) came from the 48-fin configuration, which maintained lower outlet air temperatures longer.

At 100 mm, average savings peaked at 9.06% with 48 fins, where PCM melted almost completely. However, no-fin and low-fin setups showed only marginal improvement due to insufficient heat transfer area.

Overall, energy savings initially dropped due to PCM's sensible heating but rose during the melting

phase due to latent heat absorption. After full melting, savings declined again. Thus, optimal fin number and PCM thickness are key for stable performance.

5. Conclusion

This study demonstrates that retrofitting conventional HVAC systems with a PCM-based heat exchanger can significantly reduce energy consumption by pre-cooling ambient air. Calcium Chloride Hexahydrate ($CaCl_2 \cdot 6H_2O$) was identified as the most suitable PCM based on thermal properties and TOPSIS analysis. Parametric evaluations showed that increasing PCM thickness and fin count enhances energy savings, with a 48-finned, 100 mm thick PCM heat exchanger achieving peak and average savings of 12% and 9.06%, respectively, over 6 hours of operation. The proposed system offers a practical approach for improving energy efficiency, indoor air quality, and infection control. Future work should consider real-time humidity data, varied climates, and alternative heat transfer enhancement methods to broaden the applicability of the findings.

REFERENCES

[1] G. OF INDIA, OZONE CELL MINISTRY OF ENVIRONMENT, FOREST & CLIMATE CHANGE GOVERNMENT OF INDIA MARCH, 2019, (2019).

[2] R. KUMAR SHARMA, S. YAGNAMURTHY, D. RAKSHIT, ENERGY ANALYSIS OF A PHASE CHANGE MATERIAL EMBEDDED HEAT EXCHANGER FOR AIR CONDITIONING LOAD REDUCTION IN DIFFERENT INDIAN CLIMATIC ZONES, SUSTAIN. ENERGY TECHNOL. ASSESSMENTS. 53 (2022), 102776, HTTPS://DOI.ORG/10.1016/J.SETA.2022.102776.

[3] N.H. ABU-HAMDEH, A.A. MELAIBARI, T.S. ALQUTHAMI, A. KHOSHAIM, H.F. OZTOP, A. KARIMIPOUR, EFFICACY OF INCORPORATING PCM INTO THE BUILDING ENVELOPE ON THE ENERGY SAVING AND AHU POWER USAGE IN WINTER, SUSTAIN. ENERGY TECHNOL. ASSESSMENTS. 43 (2021), 100969, HTTPS://DOI.ORG/10.1016/J.SETA.2020.100969.

[4] M. THE, E. EFFICIENCY, P. FOR, INDIA ' S ROOM AC SECTOR.

[5] R. VERMA, S. KUMAR, D. RAKSHIT, B. PREMACHANDRAN, DESIGN AND OPTIMIZATION OF ENERGY CONSUMPTION FOR A LOW-RISE BUILDING WITH SEASONAL VARIATIONS UNDER COMPOSITE CLIMATE OF INDIA, J. SOL. ENERGY ENG. 145 (2023), HTTPS://DOI.ORG/ 10.1115/1.4054831.

[6] INDIA ENERGY OUTLOOK 2021 – ANALYSIS - IEA. HTTPS://WWW.IEA.ORG/REPORTS/INDIA- ENERGY-OUTLOOK-2021 (ACCESSED SEPTEMBER 6, 2022).

[7] S. VASHISHT, D. RAKSHIT, RECENT ADVANCES AND SUSTAINABLE SOLUTIONS IN AUTOMOBILE AIR CONDITIONING SYSTEMS, J. CLEAN. PROD. 329 (2021), 129754, HTTPS://DOI.ORG/ 10.1016/J.JCLEPRO.2021.129754.

[8] V. KAPUR, B. AGARWAL, G. BALIGA, J.M. BHAMBURE, V. GARG, J. MATHUR, R. MITTAL, V. MURTHY, S. RAJASEKARAN, Y. SHUKLA, A. SUR, ISHRAE COVID-19 GUIDANCE DOCUMENT FOR AIR CONDITIONING AND VENTILATION, INDIAN SOC. HEATING, REFRIG. AIR COND. ENG. (2020) 15.

[9] WASHINGTON STATE DEPARTMENT OF HEALTH, VENTILATION AND AIR QUALITY FOR REDUCING TRANSMISSION OF COVID-19, 19 (2020) 1–4.

[10] A. SHARMA, S.K. SHARMA, T.K.M. ROHTASH, INFLUENCE OF OZONE PRECURSORS AND PARTICULATE MATTER ON THE VARIATION OF SURFACE OZONE AT AN URBAN SITE OF DELHI, INDIA, SUSTAIN. ENVIRON. RES. 26 (2016) 76–83, HTTPS://DOI.ORG/10.1016/J. SERJ.2015.10.001.

[11] A. KUMAR, S.K. SAHA, LATENT HEAT THERMAL STORAGE WITH VARIABLE POROSITY METAL MATRIX: A NUMERICAL STUDY, RENEW. ENERGY. 125 (2018) 962–973, HTTPS://DOI.ORG/ 10.1016/J.RENENE.2018.03.030.

[12] V. GOEL, A. SAXENA, M. KUMAR, A. THAKUR, A. SHARMA, V. BIANCO, POTENTIAL OF PHASE CHANGE MATERIALS AND THEIR EFFECTIVE USE IN SOLAR THERMAL APPLICATIONS: A CRITICAL REVIEW, APPL. THERM. ENG. 219 (2023), 119417, HTTPS://DOI.ORG/10.1016/J. APPLTHERMALENG.2022.119417.

[13] C. Li, B. Zhang, B. Xie, X. Zhao, J. Chen, Z. Chen, Y. Long, Stearic acid/expanded graphite as a composite phase change thermal energy storage material for tankless solar water heater, Sustain. Cities Soc. 44 (2019) 458–464, https://doi.org/ 10.1016/J.SCS.2018.10.041.
[14] S.M. Shalaby, M.A. Bek, A.A. El-Sebaii, Solar dryers with PCM as energy storage medium: A review, Renew. Sustain. Energy Rev. 33 (2014) 110–116, https://doi. org/10.1016/J.RSER.2014.01.073.
[15] S. Kumar Verma, R. Kumar, M. Barthwal, D. Rakshit, A review on futuristic aspects of hybrid photo-voltaic thermal systems (PV/T) in solar energy utilization: Engineering and Technological approaches, Sustain. Energy Technol. Assessments. 53 (2022), 102463, https://doi.org/10.1016/J.SETA.2022.102463.
[16] A. Sharma, V.V. Tyagi, C.R. Chen, D. Buddhi, Review on thermal energy storage with phase change materials and applications, Renew. Sustain. Energy Rev. 13 (2009) 318–345, https://doi.org/10.1016/j.rser.2007.10.005.
[17] C. Croitoru, I. Nastase, F. Bode, A. Meslem, A. Dogeanu, Thermal comfort models for indoor spaces and vehicles - Current capabilities and future perspectives, Renew. Sustain. Energy Rev. 44 (2015) 304–318, https://doi.org/10.1016/j. rser.2014.10.105.
[18] J. KoSny, K. Biswas, W. Miller, S. Kriner, Field thermal performance of naturally ventilated solar roof with PCM heat sink, Sol. Energy. 86 (2012) 2504–2514, https://doi.org/10.1016/j.solener.2012.05.020.
[19] R. Saxena, D. Rakshit, S.C. Kaushik, Experimental Assessment of Characterised PCMs for Thermal Management of Buildings in Tropical Composite Climate, in: MCM2018, Avestia, Madrid, Spain, 2018. https://doi.org/10.11159/htff18.170.
[20] Z. Cao, G. Zhang, Y. Liu, X. Zhao, C. Li, Influence of backfilling phase change material on thermal performance of precast high-strength concrete energy pile, Renew. Energy. 184 (2022) 374–390, https://doi.org/10.1016/J.
RENENE.2021.11.100.
[21] L. Zhu, Y. Yang, S. Chen, Y. Sun, Numerical study on the thermal performance of lightweight temporary building integrated with phase change materials, Appl. Therm. Eng. 138 (2018) 35–47, https://doi.org/10.1016/J.
APPLTHERMALENG.2018.03.103.
[22] M. Ariel, F. Bilgin, S. Nizetic, H. Karabay, PCM integrated to external building walls: An optimization study on maximum activation of latent heat, Appl. Therm. Eng. 165 (2020), https://doi.org/10.1016/j.applthermaleng.2019.114560.
[23] L.F. Cabeza, C. Castellon, M. Nogues, M. Medrano, R. Leppers, O. Zubillaga, Use of microencapsulated PCM in concrete walls for energy savings, Energy Build. 39 (2007) 113–119, https://doi.org/10.1016/J.ENBUILD.2006.03.030.
[24] M. Bahrar, Z.I. Djamai, M. EL Mankibi, A. Si Larbi, M. Salvia, Numerical and experimental study on the use of microencapsulated phase change materials (PCMs) in textile reinforced concrete panels for energy storage, Sustain. Cities Soc. 41 (2018) 455–468, https://doi.org/10.1016/J.SCS.2018.06.014.
[25] Y. Cui, J. Xie, J. Liu, S. Pan, Review of Phase Change Materials Integrated in Building Walls for Energy Saving, Procedia Eng. 121 (2015) 763–770, https://doi. org/10.1016/J.PROENG.2015.09.027.
[26] M. Xiao, B. Feng, K. Gong, Preparation and performance of shape stabilized phase change thermal storage materials with high thermal conductivity, Energy Convers. Manag. 43 (2002) 103–108, https://doi.org/10.1016/S0196-8904(01)00010-3.
[27] M. Turski, R. Sekret, Buildings and a district heating network as thermal energy storages in the district heating system, Energy Build. 179 (2018) 49–56, https://doi.org/10.1016/J.ENBUILD.2018.09.015.
[28] M. Turski, K. Nogaj, R. Sekret, The use of a PCM heat accumulator to improve the efficiency of the district heating substation, Energy 187 (2019), 115885, https://doi.org/10.1016/J.ENERGY.2019.115885.
[29] A. Lazaro, P. Dolado, J.M. Marín, B. Zalba, PCM–air heat exchangers for free- cooling applications in buildings: Experimental results of two real-scale prototypes, Energy Convers. Manag. 50 (2009) 439–443, https://doi.org/10.1016/J.
ENCONMAN.2008.11.002.
[30] N. Morovat, A.K. Athienitis, J.A. Candanedo, V. Dermardiros, Simulation and performance analysis of an active PCM-heat exchanger intended for building operation optimization, Energy Build. 199 (2019) 47–61, https://doi.org/ 10.1016/J.ENBUILD.2019.06.022.
[31] N. Stathopoulos, M. El Mankibi, R. Issoglio, P. Michel, F. Haghighat, Air-PCM heat exchanger for peak load management: Experimental and simulation, Sol. Energy. 132 (2016) 453–466,

https://doi.org/10.1016/j.solener.2016.03.030.
[32] M. Ismail, W.K. Zahra, H. Hassan, Experimental study of vapor compression refrigeration system enhanced via tubular heat exchanger incorporating single/ dual phase change materials, Case Stud. Therm. Eng. 49 (2023), 103164, https:// doi.org/10.1016/J.CSITE.2023.103164.
[33] N. Chaiyat, Energy and economic analysis of a building air-conditioner with a phase change material (PCM), Energy Convers. Manag. 94 (2015) 150–158, https://doi.org/10.1016/J.ENCONMAN.2015.01.068.
[34] M. Ismail, W.K. Zahra, S. Ookawara, H. Hassan, Boosting the air conditioning unit performance using phase change material: Impact of system configuration, J. Energy Storage. 56 (2022), 105864, https://doi.org/10.1016/J.
EST.2022.105864.
[35] M.G. Gado, H. Hassan, Energy-saving potential of compression heat pump using thermal energy storage of phase change materials for cooling and heating applications, Energy 263 (2023), 126046, https://doi.org/10.1016/J.
ENERGY.2022.126046.
[36] M. Rastogi, A. Chauhan, R. Vaish, A. Kishan, Selection and performance assessment of Phase Change Materials for heating, ventilation and air-conditioning applications, Energy Convers. Manag. 89 (2015) 260–269, https://doi.org/ 10.1016/j.enconman.2014.09.077.
[37] S. Hashemkhani Zolfani, R. Maknoon, E.K. Zavadskas, Multiple attribute decision making (MADM) based scenarios, Vilnius Gedim. Tech. Univ. 20 (2016) 101–111, https://doi.org/10.3846/1648715X.2015.1132487.
[38] S. Chakraborty, TOPSIS and Modified TOPSIS: A comparative analysis, Decis. Anal. J. 2 (2022), 100021, https://doi.org/10.1016/J.DAJOUR.2021.100021.
[39] D. Das, R.K. Sharma, P. Saikia, D. Rakshit, An integrated entropy-based multiattribute decision-making model for phase change material selection and passive thermal management, Decis. Anal. J. 1 (2021), 100011, https://doi.org/10.1016/ J.DAJOUR.2021.100011.
[40] S.F. Ahmed, N. Rafa, T. Mehnaz, B. Ahmed, N. Islam, M. Mofijur, A.T. Hoang, G. M. Shafiullah, Integration of phase change materials in improving the performance of heating, cooling, and clean energy storage systems: An overview, J. Clean. Prod. 364 (2022), 132639, https://doi.org/10.1016/J.JCLEPRO.2022.132639.
[41] R.K. Sharma, A. Kumar, D. Rakshit, A phase change material (PCM) based novel retrofitting approach in the air conditioning system to reduce building energy demand, Applied Thermal Engineering 238 (2024) 121872, https://doi.org/10.1016/j.applthermaleng.2023.121872